



HAL
open science

Lifetime modelling of fatigue crack initiation from casting defects

Marion Geuffrard, Luc Rémy, Alain Köster

► **To cite this version:**

Marion Geuffrard, Luc Rémy, Alain Köster. Lifetime modelling of fatigue crack initiation from casting defects. International conference on fracture, Jul 2009, Ottawa, Canada. 10 p. hal-00822184

HAL Id: hal-00822184

<https://minesparis-psl.hal.science/hal-00822184>

Submitted on 14 May 2013

HAL is a multi-disciplinary open access archive for the deposit and dissemination of scientific research documents, whether they are published or not. The documents may come from teaching and research institutions in France or abroad, or from public or private research centers.

L'archive ouverte pluridisciplinaire **HAL**, est destinée au dépôt et à la diffusion de documents scientifiques de niveau recherche, publiés ou non, émanant des établissements d'enseignement et de recherche français ou étrangers, des laboratoires publics ou privés.

Lifetime Modelling of Fatigue Crack Initiation from Casting Defects

M. Geuffrard¹, L. Rémy¹, A. Köster¹

¹Centre des Matériaux, Mines, ParisTech, CNRS UMR 7633, France

1. Introduction

The lifetime to initiate an engineering crack in a component is usually predicted from Coffin-Manson curves using smooth specimens for low-cycle fatigue. However this procedure has to be examined carefully when cracks initiate from defects, such as inclusions or pores that are inherited from the manufacturing process.

A special methodology has been developed for defects occurring in turbine discs made from powder metallurgy nickel base superalloys [1-3]. A probabilistic life prediction model was so built combining measurements of the distribution of defect size and a simple fracture mechanics approach to assess small crack growth, as done by Murakami [4] for high cycle fatigue. A key issue is to know whether defects should be considered as cracks of equivalent area. The investigation carried out in [1] has shown that this approximation was effective in describing fatigue life under small scale yielding.

The purpose of the present paper is to report preliminary results of such an investigation of the assessment of casting pores in aero-engine turbine blades that are cast as directionally solidified superalloy single crystals, with a [001] axis of the face centred cubic structure along the vertical direction of the blade. These blades are submitted to high centrifugal loads and thermal mechanical fatigue loading with a major stress or strain tensor component along this [001] direction. An early investigation of casting pores at fairly low temperatures (650°C) has shown that a fracture mechanics approach could be used to predict low cycle fatigue life [5-8] in notched members, that simulate the blade root. However in the airfoil, temperatures are much higher which promote creep and oxidation interactions with pure fatigue [9]. A creep oxidation fatigue damage model has been proposed based on the growth of small cracks to predict the life of single crystal superalloys under thermal mechanical loading [2,10].

Therefore an experimental investigation has been carried out on AM1 [001] single crystals, provided by Snecma, using notched tubular specimens. Specimens with a slit normal to [001] were used to investigate the growth of small through cracks. In reality a pore is better approximated by a penny shaped defect but the through crack geometry enables more accurate measurements of micro-crack growth. Tests were carried out under fully reversed strain controlled conditions at 950°C at moderate frequencies. Small crack growth data are compared with results using long cracks. A finite element analysis is made to assess local stress redistributions, and plastic strain distributions in the vicinity of the notch, using an anisotropic crystallographic viscoplastic constitutive model [11,12]. Numerical results are then used to rationalise experimental results. Consequences on life prediction are then discussed.

1. Experimental procedure

The material used in this investigation is AM1 Ni-based single crystal. Its composition is 7.8Cr, 6.5Co, 2Mo, 5.7W, 5.2Al, 1.1Ti, 7.9Ta. The two phases γ and γ' constituting this alloys are coherent. The γ phase is a matrix of FCC structure and the γ' phase ordered forms cuboidal precipitates, and 70% of the total volume. The size of γ' precipitates is about 0.5 μm .

The micro-propagation was studied using tubular specimens (Fig.1). The crystallographic orientation of the specimen was determined by a standard Laue Back-reflection technique in order to machine the specimens with the [001] orientation. A notch, perpendicular to the specimen axis, was machined with the orientation [110]. To simulate the aspect ratio of a pore, the length of the notch is $2a_0=0.5$ mm and the root is semi-circular with a radius $r=0.05$ mm. The fatigue tests were conducted on a servo-hydraulic fatigue-testing machine at 950°C under axial strain control (triangular wave form, frequency 0.05Hz and 1Hz). All tests were run in air, with a strain ratio $R\epsilon=-1$. Cracks growth was monitored using a potential drop between two fixed points of the notch, which was calibrated using optical measurements with a camera centered on the notch.

After completion of the experiments, the crack path on the specimen surface was observed in a scanning electron microscope (SEM).

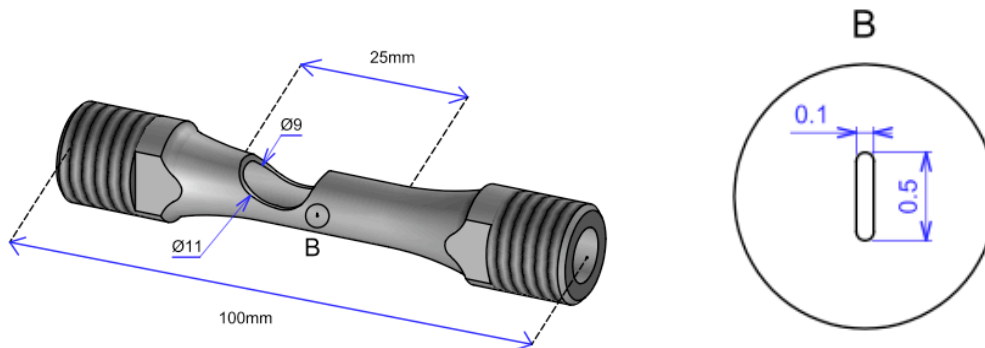


Figure 1. Specimen geometry used for crack propagation and details of notch geometry (specimen axis is [001] and notch orientation is along $\langle 110 \rangle$ direction.)

2. Experimental results

The fatigue crack growth rate (FCGR) is shown as a function of crack length a , for tubular specimen with a horizontal notch and crack growth curves are shown in Fig. 2. A very high growth rate is observed in the early stage of crack growth from the notch up to 0.15 mm from the notch tip for tests conducted at the lowest strain range. Then the crack growth rate seems to decrease and shows a minimum in the range of crack depth between 2 and $3a_0$. Actually this minimum is very shallow at the higher strain range. Then the crack growth rate increases with increasing crack length as usually observed. The same FCGR data are plotted as a function of the nominal stress intensity range for notched tubular specimen (Fig. 3), considering the notch as an initial crack, and for CT specimen tested by N. Marchal [13] at 950°C at a frequency of 0.05Hz and with a load ratio of $R=0.1$.

The present tests are conducted under push-pull conditions. Therefore only positive stress was used estimating the stress intensity factor range. An equivalent crack length was taken as the notch depth added to physical crack depth at the notch root. Comparison with long crack data from CT specimens shows, that when the crack is deep enough ($a > 3a_0$), the short cracks tend to behave like a long crack.

The surface of tubular notched specimen was observed by scanning electron microscopy (Fig. 3). The crack initiates at notch root, almost at mid-height, and the crack path is straight and perpendicular to the loading direction. This suggests, as in early studies [9], that crack initiation and growth from the notch is mostly governed by maximum principal stress or stress range. Oxidation can be quite significant at the surface especially at the higher strain range. Test data from early work [14] shows that FCGR under vacuum and at high frequency on long crack appears as a base line, in the absence of any interaction with oxidation.

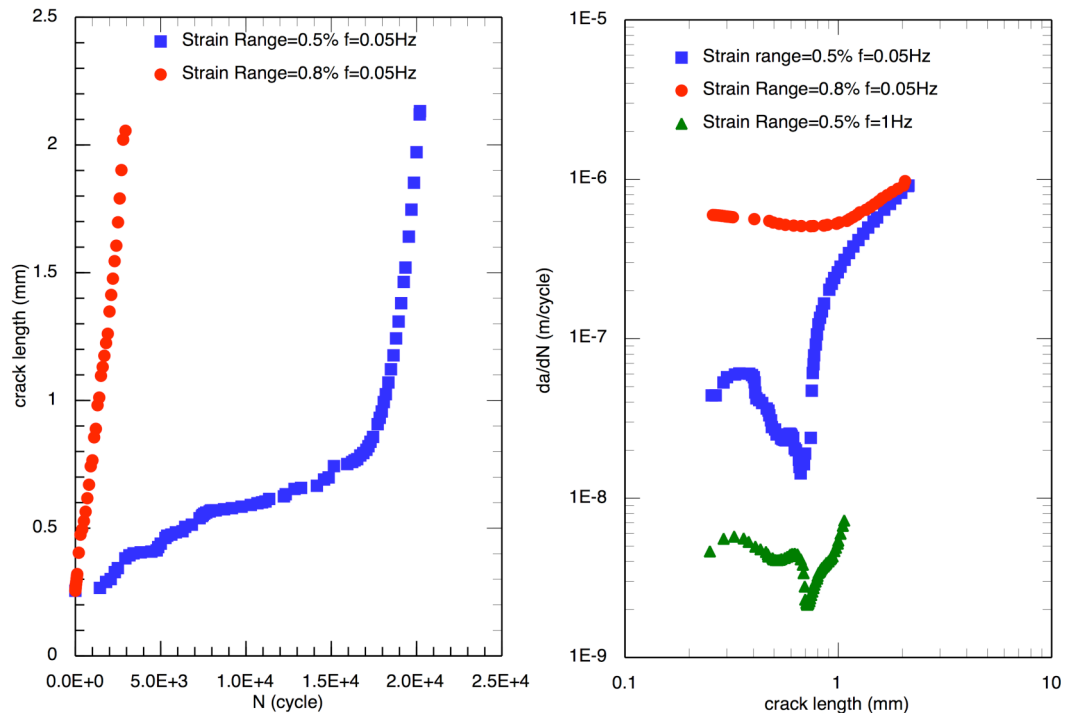


Figure 2. Effect of strain range and test frequency on crack growth curves (on the left) and on crack growth rates (da/dN) as a function of nominal crack length (on the right). ($[001] \langle 110 \rangle$ specimen, notch normal to loading axis).

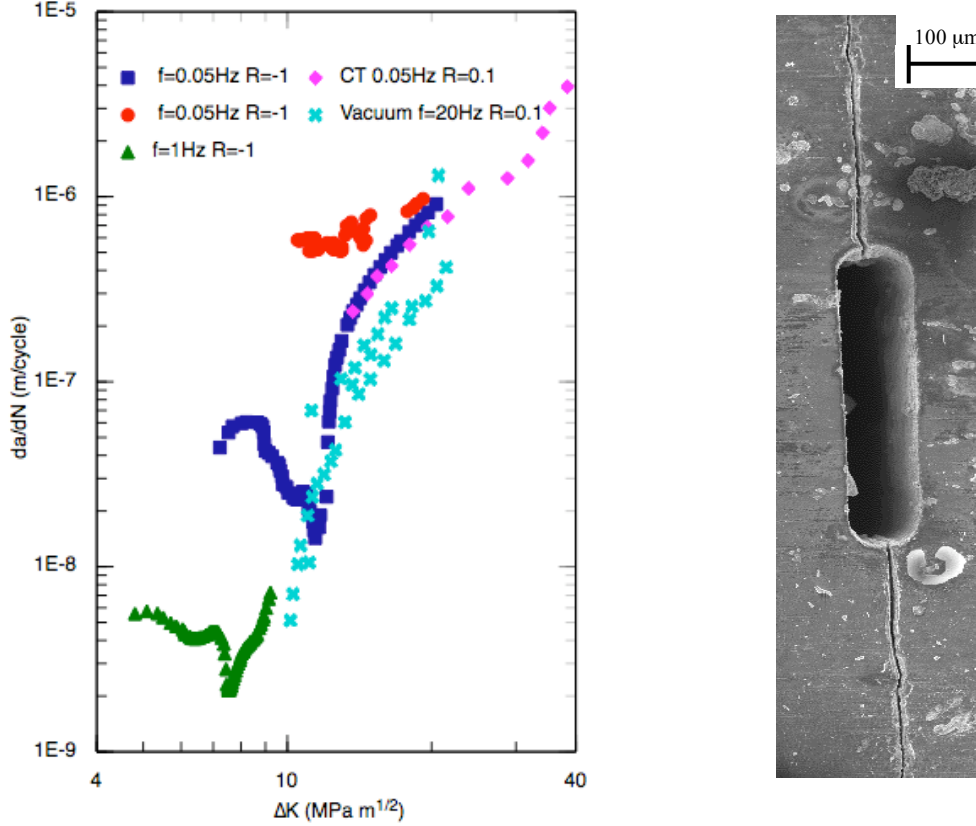


Figure 3. Effect of strain range and test frequency on crack growth rates (da/dN) as a function of range of stress intensity factor. ([001] <110> specimen, notch normal to loading axis) (on the left). Crack path from the initial notch : specimen tested at 0.5% strain range, 0.05 Hz (on the right).

3. Discussion

3.1. Constitutive behaviour

To account for the crystallographic nature of the alloy, a crystallographic constitutive law has been chosen to simulate the high temperature behaviour, proposed by Méric and Cailletaud [11]. In the present case, the model should be able to describe the situation at the crack tip, using a limited number of material parameters to reduce computation time. Strain-controlled cyclic tests were carried out at 950°C on a hydraulic fatigue machine [12]. Two sets of material parameters are used for octahedral slip systems and cube slip systems respectively. The flow rule is a Norton rule with threshold (Eq. 1):

$$\dot{\gamma}^s = \left\langle \frac{|\tau^s - x^s| - r^s}{k_I} \right\rangle^{n_I} \text{sgn}(\tau^s - x^s) \quad (1)$$

where $\dot{\gamma}^s$ and τ^s are respectively the slip rate and the resolved shear stress on slip system s . r^s and x^s are respectively the isotropic and kinematical hardening terms (here, r^s is considered constant, because there is no cyclic hardening or softening

at this temperature). k_I and n_I are two adjustable parameters, taking different values for octahedral or cube slip systems (I subscript). Non-linear kinematical hardening is considered here, as presented in equations 2 and 3.

$$x^s = c_I \alpha^s \quad (2)$$

$$\dot{\alpha}^s = \dot{\gamma}^s - d_I \dot{\gamma}^s \alpha^s \quad (3)$$

with $\dot{\gamma}^s = |\dot{\gamma}^s|$. α^s is the internal variable associated to non linear kinematical hardening. c_I and d_I are two adjustable parameters.

For macroscopic models it is usually convenient to use plot of von Mises stress and plastic strains. In the case of a single crystal, the occurrence of viscoplasticity is better described using variables that describe the activity on the slip planes, such as cumulative octahedral and cube slip variables as proposed in recent studies [14].

3.2. Finite element analysis

The 3D mesh used is representative of a notched tubular specimen with a notch orientation (001) [110]. The calculation is done using displacement controlled conditions at two nodes, as experimentally done using the strain gauge extensometer. Simulations were performed with FE code Z-set, developed at Ecole des Mines de Paris, ONERA and Northwest Numerics (www.numerics.com). The mesh is a free mesh using quadratic elements except near the notch area (Fig. 5). The calculations are done under a small strain assumption.

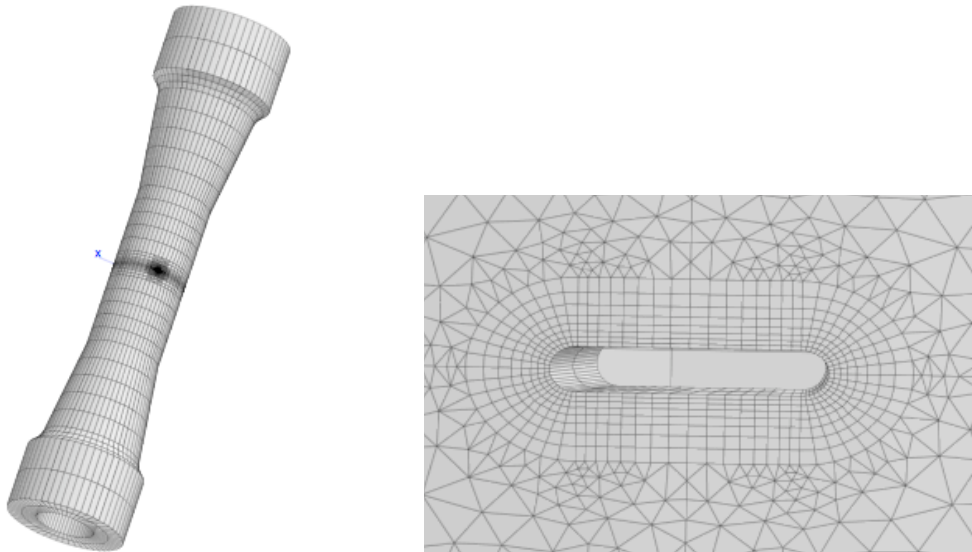


Figure 5. FE mesh : general view and details of the notch area.

A map of the cumulative octahedral slip γ_{cum}^{oct} is plotted in Fig. 6, for a test frequency 0.05Hz at maximum tensile strain. Plasticity occurs at the mid plane of the notch and tends to show a larger extension at some angle ahead of the notch. When the cumulative strain decreases, plastic strain contours look more like those observed at cracks with a maximum extension at 70-80° from the notch plane. The variation of cumulative octahedral slip is plotted as a function of distance ahead of the notch tip x , in Fig. 6. The viscoplastic strain vanishes only at 0.15mm ahead of the notch. The same computation has been carried out at 1Hz. The increase in frequency reduces the extent of plasticity ahead of the notch: maximum cumulative strain is smaller and the viscoplastic zone is smaller.

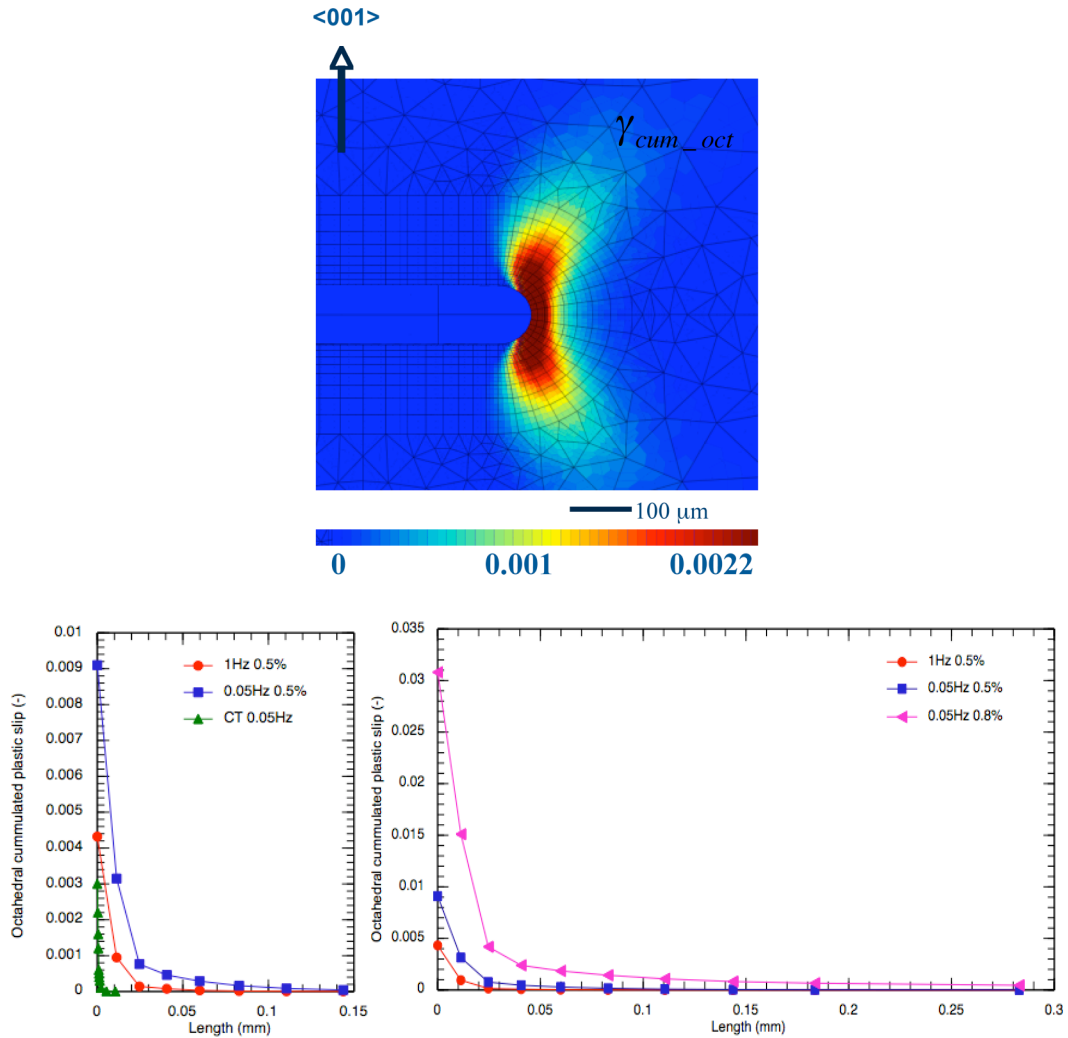


Figure 6. FE computation of the stress strain field at the notch tip (0.5% strain range, 0.05 Hz): map of octahedral cumulated plastic slip at maximum load at the notch tip (top) and as a function of distance compared with a crack tip (bottom).

3.3. Fracture mechanics analysis

Conventional linear elastic fracture mechanics is widely used to analyse crack growth in fatigue under small scale yielding conditions. In the presence of a stress gradient, one can avoid a complete determination of actual solutions for stress intensity factor using a weighting function method and an elastic or viscoplastic analysis of the non-cracked structure. If $\Delta\sigma_{33}$ is stress range normal to the crack plane, along the crack face, ΔK is given by Eq. 4:

$$\Delta K = (2/\pi)^{1/2} \int_0^a \Delta\sigma_{33}(x/a) x^{-1/2} m(x/a) dx \quad (4)$$

Where x is the distance along the crack, a the crack length, $\Delta\sigma_{33}(x/a)$ the range of normal stress as computed without crack and $m(x/a)$ a weighting function as computed by Bueckner [16,17].

This solution has been computed using results of the FE analysis. This evolution of K_{max} is shown using an elastic analysis as well as the viscoplastic model for two loading frequencies 0.05Hz and 1Hz, in Fig. 7. This figure shows too the variation of nominal K using a regular formulation considering the equivalent crack length as the sum of the notch depth and of physical crack length. Fig. 7 shows that K_{max} computed according to the weight function increases drastically between 0.25 and 0.4 mm equivalent crack depth. Then it remains lower than an equivalent crack with no stress gradient up to 0.8mm where the difference between solutions becomes very small. Results for the larger strain range are similar (Fig. 7).

This analysis explains the extent of the crack growth rate anomaly up to 0.8mm crack depth but it does not provide a convincing rationale of the very high FCGR near the notch tip, and it does not explain the decrease of FCGR down to a minimum. One may seek an effect of transient crack closure building up progressively in the wake length as proposed earlier [18].

The initial high FCGR regime seems to be related to the large viscoplastic strain occurring at the notch tip. This is shown in Fig. 6, using the cumulative plastic strain on all octahedral slip systems, which extends up to 0.15mm (at 0.05Hz) and 0.06mm (at 1Hz) ahead of the notch tip. The strain gradient is steeper for a long crack but the extent ahead of the crack as computed by Marchal [15] is much shorter for comparable loading conditions. The high initial FCGR rates scale directly with the viscoplastic cumulative strain as shown by the analysis of frequency. Local fracture criteria such as proposed recently should provide a quantitative description of the high FCGR regime [19] but they have to be identified for the present conditions since they need calibration for a given mesh size. This description is underway.

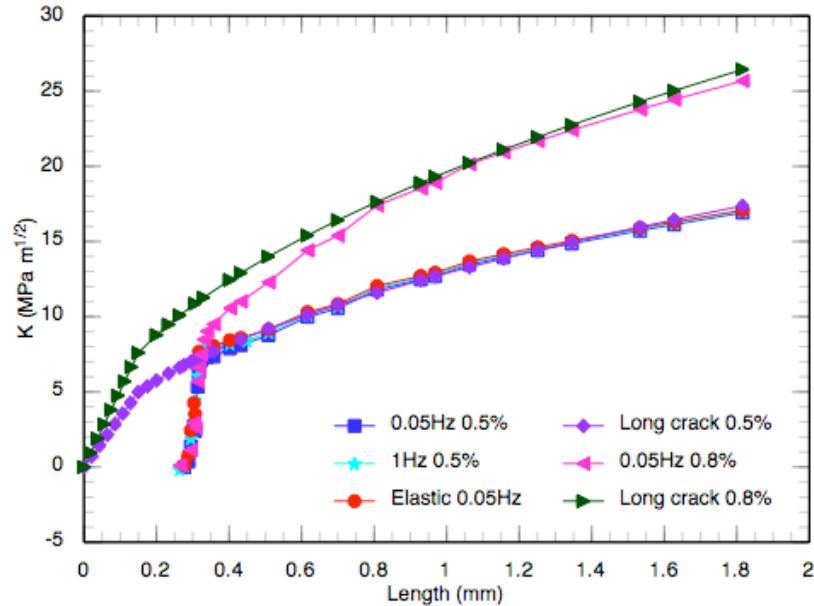


Figure 7. Maximum stress intensity factor as a function of crack depth, computed from Eq. using the maximum normal stress in the mid plane ahead of the notch FE (0.5% strain range, 0.05 Hz , 1Hz and 0.8%, 0.05Hz)).

4. Conclusions

In this paper, we have used fatigue experiments on notched specimens under tension compression fatigue at 950°C to investigate the role of casting defects in anisotropic nickel base superalloys single crystals.

A transient fatigue crack growth regime has been evidenced that extends up to about 3 times the notch depth, at low frequency, for (001) [110] notches. A 20 times increase in frequency results in a 10 times decrease of growth rate in this transient regime.

A 3D finite element model using crystallographic viscoplastic constitutive equations has shown a significant local plasticity along the slip systems. The local viscoplasticity along slip systems accounts for the high fatigue crack growth rates at notch tip. The interaction with oxidation effects remains to be assessed.

A weight function method has been used to estimate the range of stress intensity factor. This analysis provides an estimate of the area affected by the presence of the notch below which a defect cannot be treated as equivalent to a crack. However this analysis does not provide any rationale for the decrease of crack growth rate observed.

The anomalous behaviour will be investigated using a more precise FE model of cracks emanating from notches.

Acknowledgements

Financial support as well as provision of superalloy single crystals by Snecma, Safran Group, is gratefully acknowledged.

References

- [1] J. Grison and L. Rémy, Fatigue failure probability in a powder metallurgy Ni-base superalloy, *Engineering Fracture Mechanics*, vol. 57, 1997, pp. 41-55.
- [2] L. Rémy, N. Haddar, A. Alam, A. Koster, N. Marchal, « Growth of small cracks and prediction of lifetime in high temperature alloys », *Materials Science and Engineering A*, vol. 468-470, 2007, pp 40-50, doi: 10.1016/j.msea.2006.08.133.
- [3] J.C. Lautridou, J.Y. Guédou and Y. Honnorat, Effect of inclusions on LCF life of PM superalloys for turboengines discs. *High Temperature Materials for Power Engineering 1990*, ed. E. Bachelet et al., 1990, pp. 1163-1172.
- [4] Y. Murakami and M. Endo, Effects of defects, inclusions and inhomogeneities on fatigue strength. *Fatigue*, 1994, 16, 163-182.
- [5] A. Defresne, L. Rémy, "Fatigue behaviour of CMSX2 superalloy [001] single crystals at high temperature. I : Low cycle fatigue of notched specimens", *Materials Science and Engineering*, vol. A 129, 1990, pp.45-53.
- [6] A. Defresne, L. Rémy, Fatigue behaviour of CMSX 2 superalloy [0 0 1] single crystals at high temperature II: fatigue crack growth, *Materials Science and Engineering A 129 (1990) 55–64*.
- [7] A. Defresne, L. Rémy, "Fatigue life prediction of notched specimens of nickel based superalloy single crystals", *Fatigue 90, Proceedings of the fourth International Conference on Fatigue and Fatigue Thresholds, July 15-20 1990, Honolulu (Hawaii)* H. Kitagawa, T. Tanaka, Eds, *Materials and Component Engineering Publications*, Edgbaston, 1990, vol.4, pp.2435-2440.
- [8] L. Rémy, Application of fatigue crack growth data to low cycle fatigue at high temperature, in: *Handbook of fatigue crack propagation in metallic structures*, Ed. Andrea Carpinteri, 1994, Elsevier, pp.1307-1346.
- [9] E. Fleury, L. Rémy, "Low cycle fatigue damage in nickel-base superalloy single crystals at elevated temperature", *Materials Science and Engineering*, vol. A167, 1993, pp.23-30.
- [10] A. Köster, A.M. Alam, L. Rémy, A physical-base model for life prediction of single crystal turbine blades under creep-fatigue loading and thermal transient conditions, in: *Temperature–Fatigue Interaction*, in: L. Rémy, J. Petit (Eds.), *ESIS Publication 29*, Elsevier, Paris, 2002, pp. 203–212.
- [11] Méric, L., P. Poubanne, and G. Cailletaud (1991). *Single Crystal Modelling for Structural Calculations: Part 1 - Model Presentation*. *Journal of Engineering Materials and Technology*. 113, 162.
- [12] F. Hanriot, G.Cailletaud, L. Rémy, Mechanical behaviour of a nickel base superalloy single crystal, in "High temperature constitutive modeling. Theory and application", Eds. A.D. Freed and K.P. Walker, *American Society of Mechanical Engineers*, New-York, USA, MD-Vol.26/AMD-Vol.121, 1991, pp.139-150.

- [13] N. Marchal, Propagation de fissure en fatigue-fluage à haute température de superalliage monocristallins à base nickel. Ph.D. thesis. Centre des Matériaux, Ecole Nationale Supérieure des Mines de Paris, (2006) pp 98.
- [14] E. Fleury, Endommagement du superalliage monocristallin AM1 en fatigue isotherme et anisotherme. Ph.D. thesis. Centre des Matériaux, Ecole Nationale Supérieure des Mines de Paris, (1991).
- [15] N. Marchal, S. Flouriot, S. Forest, L. Rémy, « Crack-tip stress-strain fields in single crystal nickel-base superalloys at high temperature under cyclic loading », Computational Materials Science, vol. 37 (2006), pp. 42-50.
- [16] H.F. Bueckner, Field singularities and related integral representations, in Mechanics of fracture, G.C. Sih, Ed., Nordhoff, Leyden, 1973, vol.1, pp.239-314.
- [17] H.F. Bueckner, Weight functions and fundamental fields for the penny shaped and the half plane crack in a 3 space, Int. J. Solids, vol. 23, 1987, pp. 57-93.
- [18] K. Minakawa, J.C. Newman and A.J. McEvily, A critical study of the crack closure effect on near threshold fatigue crack growth. Fatigue of Engin. Mat. and Struct., 6, 1983, pp. 359-365.
- [19] N. Marchal, L. Rémy, S. Forest, S. Duvinage, « Crack propagation in single crystal nickel base superalloys under creep-fatigue loading conditions », Fatigue 2006, 9th International Fatigue Congress, 2006, May 14-19, Atlanta, Georgia Tech, Elsevier, CD - Rom, 10p.